Ecological features and swimming capabilities of deep-sea sharks from New Zealand

Nicolas Pinte, Pascaline Parisot, Ulrich Martin, Vincent Zintzen, Christophe De Vleeschouwer, Clive D. Roberts, Jerome Mallefet

A B S T R A C T

Currently the ecology of deep-water sharks is poorly documented, especially *in situ* information for these elusive species are lacking. In this study, stereo-Baited Remote Underwater Videos (stereo-BRUVs) were deployed to collect ecological data from New Zealand deep-sea sharks. The results showed differences in abundance between species, with *Etmopterus granulosus* (Etmopteridae) found in greatest numbers. Moreover, the known depth range increased for *Scymnodon macracanthus* (Centrophiridae). Deep-sea shark species were generally found to swim at slower cruise speeds (0.36 ± 0.04 m s^{-1}) than their shallow-water counterparts (0.63 ± 0.05 m s^{-1}). However, the swimming speed of deep-sea sharks was clearly not uniform, with some species displaying higher cruise swimming speeds than others. The fastest sharks (*Centrophorus harrissoni*, *Etmopterus granulosus* and *Etmopterus molleri*) had swimming abilities comparable to benthic shallow water sharks (0.48 ± 0.02 m s^{-1}). The higher cruise swimming speed in the family Etmopteridae could be an advantage for these luminous sharks if they follow isolumes to match their ventral light intensity with the down-welling light of their environment. This study revealed that alternative non-destructive methods can be effective for ecological studies of deep-sea marine fauna.

1. Introduction

We still know very little about the ecology of deep-sea sharks. They live at depths characterized by high pressure, darkness, low temperature and low oxygen concentration, which are factors making life observations of specimens difficult (Chiswell et al., 2015; Gallo et al., 2014). Few studies identified some key elements of the basic ecology for some of these species (Finucci et al., 2018; Coelho and Erzini, 2010; Andrews et al., 2009; Clarke et al., 2002; Girard and Du Buit, 1999; Nelson et al., 1997).

One important aspect that has not yet been very well studied is the swimming capabilities of deep-sea sharks. The swimming capability of an organism in the ocean has essential implications in survival behaviors such as hunting, escaping, migrating, and mating (Watanabe et al., 2012; Wilson et al., 2005). Swimming capability will also largely dictate the home range of a species (Sainte-Marie and Hargrave, 1987). Shadwick et al. (2016) split the swimming speeds of fishes into two main types: The first is linked to burst activities – when fishes reach their maximum velocity quickly during hunting or escaping behaviors. The second is linked to cruise activities, and is used by fishes to travel long distances during the most common locomotion activities such as foraging, dispersal, locating a mate or circadian migration (Ryan et al., 2015; Watanabe et al., 2012).

Swimming capabilities studies of shallow-waters species showed that elasmobranchs possess a large diversity of morphological, anatomical and physiological adaptations linked to their locomotion system (Lauder and Di Santo, 2015; Shadwick and Goldbogen, 2012; Gemballa et al., 2006; Bernal et al., 2003; Thomson and Simanek, 1977). In contrast, few studies have looked at swimming behaviors of deep-water sharks. These sharks are often described as slow and listless swimmers (Condon et al., 2012; Treberg et al., 2003; Bagley et al., 1994), as for the Greenland shark recorded as the slowest (Watanabe et al., 2012) but some of them still perform long vertical migration such as *Centrophorus squamosus* (Rodríguez-Cabello et al., 2016; Rodriguez and Sanchez, 2014). Two

main hypotheses have been put forward to explain this. The first is that cold water directly affects the muscular contraction metabolism of these ectothermic fishes (Treberg et al., 2003). The second, called the visual interaction hypothesis (VIH), suggests that declining light levels with depth decreases the selective pressure for efficient locomotor capacity by species with visual capabilities, because the reactive distances between predator and prey are reduced (Condon et al., 2012). The majority of data about the swimming performance of deep-sea sharks have so far been inferred indirectly from measurements of their metabolisms (Condon et al., 2012; Treberg et al., 2003). These two studies have shown that anaerobic metabolism is lower for deep-sea species than their shallow-water counterparts while no difference is observed for the aerobic metabolism.

In our study, we evaluated the occurrence and relative abundance of sharks on the slopes off New Zealand at depths from 300 to 1200 m at latitudes of 29.15–50.91°S using stereo-BRUVs. These deployments enabled to measure ecological features such as the size, the swimming speed and the tail-beat frequency of eight deep-sea shark species. The results obtained allow us not only to compare absolute values of cruise swimming speeds of deep-sea sharks with cruise swimming speed values of shallow-water species found in the literature; but also to study the difference in cruise swimming speeds and tail beat frequency between the deep-sea species.

2. Materials and methods

2.1. Video recording

Video deployments were carried out in New Zealand waters between 2009 and 2012 during daylight of the austral summer months (see Zintzen et al., 2012, 2017 for details on video deployments). The videos were recorded at seven different locations spanning a latitudinal range between 29.15°S and 50.91°S, at five different depths (300, 500, and 700, 900 and 1200 m) at each of these locations. A minimum of six video replicates were achieved at each depth by location cell, yielding a total of 247 deployments. The camera systems were stereo-baited remote underwater video systems (stereo-BRUVs) that included two Sony Handycam HD cameras of the models HDR-CX7 or HDR-CX500. They were placed 70 cm apart on the base bar with an 8° rotation toward the central bait. Each system was illuminated using Royal Blue Cree XLamps XP-E LEDs. Parameters were selected to provide sufficient vision range (clearly observed until five meters from cameras) and minimizing fish repulsion, backscatter, and light reflection from silvery fishes (Zintzen et al., 2012, 2017). Ten additional red LED lamps, to enable the synchronization of the right and left cameras, were placed in the vision field of the two cameras and turned on one after one regularly during the whole recording period.

2.2. Shark identification and general ecological features

Sharks were identified in the high definition digital images coupled with large fish traps deployed simultaneously to the video systems, to capture voucher specimens. Species level identifications were based on Roberts et al. (2015) and Ebert et al. (2013).

Following shark identification, we measured species richness according to the depth, which is defined as the number of different species of sharks for a particular depth stratum (300, 500, 700, 900, and 1200 m) (Zintzen et al., 2012). We also evaluated the relative abundance of each squaliform family. For that purpose, we distinguished and counted individuals for each family over the course of the deployment. Then, we reported this number according to the total number of sharks observed. Length (total, fork, and precaudal length) was also measured and aggregation was assessed to determine if some species occurred in large numbers, or were singletons. For this purpose, all individuals of each species were counted over the course of each deployment.

2.3. Swimming speed and tail beat frequency

The swimming speed and length values were measured using MatLab software (MATLAB and Statistics Toolbox Release, 2012b, The MathWorks, Inc., Natick, Massachusetts, United States). A short summary of the method is given below.

Pairs of video cameras were calibrated using a calibration cuboid ($1000 \times 1000 \times 500$mm with high contrast white spots) in a swimming pool. The first step was the modeling of the cuboid and its spots in MatLab. For that, each spot was converted as a number and related with 3D coordinates. Then, a MatLab code was developed to calibrate cameras by associating each spot from the right and the left images with their matching spots using the pinhole camera model. This method provided parameters of each of them for next measurements. (Hartley and Zisserman, 2004; Heikkilä, 2000; Zhang, 1999; Heikkilä and Silken, 1997).

For size and speed measurements, we needed to measure the "x, y" shark coordinates in pixels for the left and right images. For the size, four specific points representing total, fork and precaudal lengths were selected (rostrum, precaudal pit, posterior notch and terminal margin). For velocity, three points visible on the videos from the left and the right cameras were selected along the body. The use of three different points allows accounting for speed differences in function of the selected point. For example, if one point is the rostrum, a left or right movement of the head will change the distance travelled every few seconds. One image per second was extracted to measure the swimming speed of a shark during its displacement. The points selected on the body of the shark remained identical through the entire sequence. The 2D coordinates of the body of the shark obtained with MatLab were inserted into another MatLab code. This new code converted the 2D coordinates of each point into 3D coordinates, thanks to the calibration matrix of the stereo-camera systems. With the coordinates in three-dimensions, it was possible to measure the size and speed of a shark by taking the vector length between the points. Measurement repeatability was estimated by measuring several times the LED synchronization lamp and the error of measurement was calculated to 0.91 cm.

The speed recorded was classified in two categories: (i) burst swimming speed when acceleration of shark was identified due to predation or predation avoidance behaviors; when such behaviors are not observed we considered burst speed to be when speed excess 6 to 18 body length s^{-1} (Ryan et al., 2015). And (ii) the cruise swimming speed when the shark swam without any interaction with other organisms or the BRUVs system. Therefore, sharks swimming with a direct bait interest (touching, smelling, and biting) were not taken into account.

To determine whether swimming species of deep-sea sharks differ from their shallow-water counterparts, the swimming speed values obtained in our study were compared with similar results from compiled literature (Ryan et al., 2015; Watanabe et al., 2012) (Supplementary data 1). We used these velocity values for comparison because they were collected using the same criteria as ours: (i) measurements were obtained during day time, and (ii) only on mature individuals. A total of 20 shallow-water sharks and a deep-water one, grouped in six different orders were compiled. Sharks were classified in general groups: surface (i.e., living most of their time above 200m depth) and deep (i.e., living most of their time deeper than 200m). A second deeper classification was defined according to the habitat of surface sharks (pelagic or benthic) and the velocity groups obtained by the first test for deep-sea sharks.

Finally, for each velocity value obtained, we measured the corresponding tail beat frequency. Tail beat frequency is defined as the time required for the tail to move from one extreme lateral position back to the same position and it is expressed in Hertz (Hz). In this study, the tail beat frequency was calculated from the time difference between the two images corresponding to this complete motion (Watanabe et al., 2012). Thanks to the speed and tail beat frequency, it is also possible to measure the stride length (corresponding to the ratio of the speed to the tail beat

frequency, expressed as a fraction of body length) for each species at a given speed (0.3 m s^{-1}). This speed was chosen because it is the speed common to almost all species except *Dalatias licha*, which never reached this speed.

2.4. Statistical analyses

All statistical analyses (univariate parametric and non-parametric tests) were performed with JMP pro 14 (JMP®, Version <14>. SAS Institute Inc., Cary, NC, 1989–2007). The normality and the homoscedasticity were confirmed for each parametric test. When the Gaussian distribution was not proved, non-parametric equivalent tests were used.

3. Results

3.1. Video analyses

The 267 h of video recording allowed more than 1400 shark observations (number of shark individuals observed) to be made. Twenty-eight species of sharks from three orders (Carcharhiniformes, Hexanchiformes, and Squaliformes) were identified (Table 1). Eight deep-sea shark species (*Dalatias licha*, *Centroscymnus owstonii*, *Proscymnodon plukenti*, *Centrophorus squamosus*, *Centrophorus harrissoni*, *Deania calcea*, *Etmopterus granulosus*, and *Etmopterus molleri*) were common enough in video recordings to enable accurate swimming speed measurements. Of these, a total of 253 speed measurements and 135 size measurements were obtained, with a minimum of seven measurements of swimming speed for each species. The lower number of size measurements is explained by frames where individuals were not entirely visible as for some bigger sharks, such as the bluntnose sixgill shark (*Hexanchus griseus*), which were common enough, but too large for the camera field of view.

3.2. Biodiversity analyses

Species richness of sharks changed with depth (Fig. 1A). The number of species from all locations was ten at 300 m and increased to reach a maximum of twelve species at 700 m. It then decreased to ten species at 900 m, and six species at 1200 m. At the two shallower depths (300–500 m), three orders were represented. Deeper (700–900 m) Carcharhiniformes disappear, but at the greatest depth studied (1200 m) one Carcharhiniformes species (*Apristurus* sp.) was found. Squaliformes was the most represented order in the deep water (i.e. under 200 m depth), and accounted for 91% of all shark observations.

Family analysis of Squaliformes showed that at 300m, 98% of sharks were Squalidae, with the rest belonging to Somniosidae, Etmopteridae and Oxynotidae (Fig. 1B). Between 500 and 900m, Etmopteridae individuals were the most represented group, with a stable relative abundance across the range of 44%. The proportion of Squalidae individuals decreased with depth (40% at 500m, 16% at 700m, 2% at 900m), while the proportion of Centrophoridae and Somniosidae individuals increased (2% and 13% at 500m, 12% and 29% at 700m, 19% and 28% at 900m, respectively). In the deepest layer (1200m), Etmopteridae represented 76% of all sharks observed, while the percentage of Centrophoridae and Somniosidae decreased to 1% and 23%, respectively.

Table 1
Summary of data collected on the 28 species of sharks observed from stereo-baited underwater video surveys in New Zealand EEZ; total number of individual observations (# obs), number of replicate for size measurement (n1), mean total length ± SE (TL cm), number of replicate for speed measurement (n2), cruise swimming speed (CS m.s^{-1}) and burst swimming speed (BS m^{-1}). * Luminous shark based on our observations and literature. Taxa classification is based on Roberts et al. (2015) and Ebert et al. (2013).

Order Family Species	# obs	Depth range (m)	n1	TL (cm)	n2	CS (m s^{-1})	Burst (m s^{-1})
Squaliformes							
Dalatiidae							
*Dalatias licha**	27	300–900	10	110.82 ± 22.59	22	0.13 ± 0.04	
Somniosidae							
Centroscymnus owstonii	84	700–1200	6	97.96 ± 19.22	19	0.29 ± 0.10	1.03
Centroscymnus coelolepis	2	900	–	–		–	–
Centroselachus crepidater	2	700–900	–	–		–	–
Proscymnodon plukenti	264	300–1200	26	121.76 ± 29.64	38	0.32 ± 0.11	1.32
Scymnodon macracanthus	13	300–900	–	–		–	–
Centrophoridae							
Centrophorus squamosus	55	500–900	24	134.80 ± 13.49	37	0.32 ± 0.07	0.76
Centrophorus harrissoni	115	500–900	14	78.95 ± 7.75	35	0.53 ± 0.17	
Deania calcea	69	500–900	8	79.69 ± 13.86	20	0.33 ± 0.12	
Etmopteridae							
*Etmopterus granulosus**	759	500–1500	45	52.60 ± 13.45	61	0.45 ± 0.14	1.59
*Etmopterus molleri**	21	300–700	2	38.15 ± 1.87	7	0.51 ± 0.14	
*Etmopterus lucifer**	2	1200	–	–		–	–
Oxynotidae							
Oxynotus bruniensis	1	300	–	–	–		
Squalidae							
Squalus acanthias	12	300–600	–	–	–		
Squalus griffini	13	300–700	–	–	–		
Cirrhigaleus australis	6	300–700	–	–	–		
Carcharhiniformes							
Scyliorhinidae							
Cephaloscyllium isabellum	11	300	–	–	–		
Galeorhinus galeus	9	300	–	–	–		
Bythaelurus dawsoni	2	300	–	–	–		
Parmaturus sp.	3	1200	–	–	–		
Apristurus sp.	1	900	–	–	–		
Hexanchiformes							
Hexanchinidae							
Hexanchus griseus	24	300–900	–	–	–		

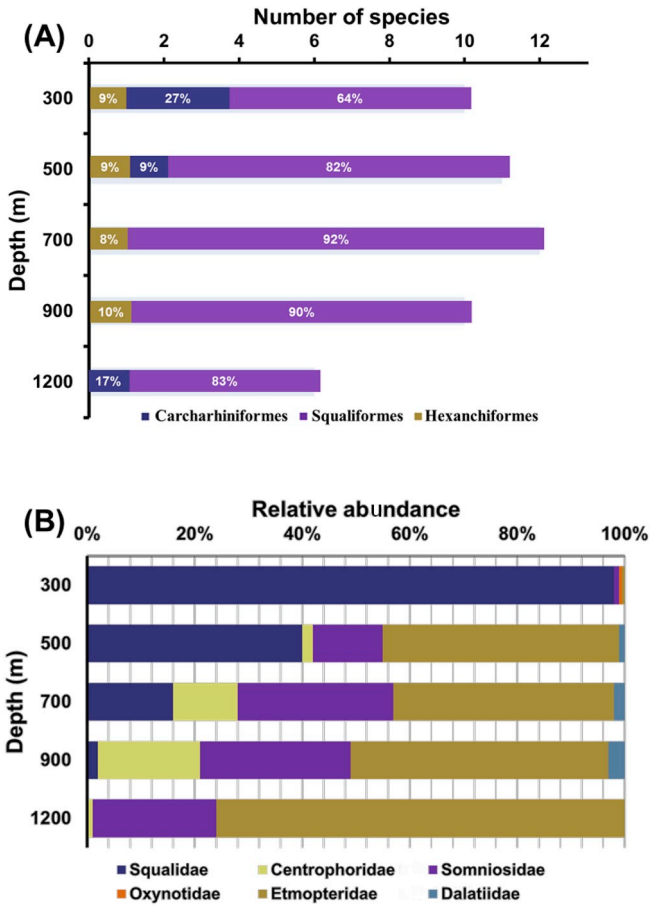

Fig. 1. (A) Shark species richness according to depth, observed from video deployments. Percentage indicates the proportion of the total number of shark observations within the four orders of sharks identified. (B) Relative abundance of families of Squaliformes according to depth. The percentage represents the proportion of all the specimen observations belonging to one of six families.

3.3. Length analyses

The relationship between total length of each shark species and depth revealed no significant difference (ANOVA, $P > 0.05$); except for *C. harrissoni* (see Supplementary Data 2). However, three different distribution patterns were observed: (i) sizes greater at shallower and deeper depths, with intermediate values in mid depth range, found for *C. owstonii* and *P. plukenti*; (ii) longer specimens measured in deep waters, found for *C. harrissoni* and *D. calcea* and (iii) sizes decreasing progressively with depth for *E. granulosus* and *C. squamosus*. Regarding *Dalatias licha* and *Etmopterus molleri* no relation could be done due to the lack of occurrence at different deep layers.

3.4. Aggregation pattern

Results showed that *E. granulosus* occurred in much larger numbers (12.35 ± 1.04 individuals) than other species (average for all other species: 3 ± 0.69 individuals) (Kruskal-Wallis test, $P < 0.0001$) (see bar chart representing these values in Supplementary Data 2).

3.5. Swimming speed

There were statistically significant differences between cruise swimming speeds of the eight deep-sea shark species (Welch test, $P < 0.0001$) (Fig. 2). Paired comparison isolated three significant groups (Tukey test, $P < 0.01$). The first group comprised just *D. licha*, displaying the slowest cruise swimming speed (group deep A: 0.13 ± 0.01 m s^{-1}). The second group was represented by *C. owstonii*, *P. plukenti*, *C. squamosus* and *D. calcea* having intermediate cruise swimming speeds (group deep B: 0.31 ± 0.01 m s^{-1}). The last group, with *E. granulosus*, *E. molleri* and *C. harrissoni*, showed the highest cruise swimming speeds (group deep C: 0.48 ± 0.02 m s^{-1}) (Fig. 2).

Comparison between deep-sea shark species and shallow-water ones from the literature showed a significant difference in cruise swimming speed (Student *t*-test, $P < 0.0012$), with shallow-water sharks displaying higher cruise swimming speeds ($n = 20$, 0.63 ± 0.05) than deep-sea sharks ($n = 9$, 0.36 ± 0.04) (Fig. 3).

Looking into the details of this difference between shallow and deep-water species revealed that not all deep-water sharks have slower cruise swimming speeds than their shallow counterparts (Fig. 4). There were significant differences between cruise swimming speeds of pelagic shallow-water sharks, benthic shallow-water sharks, and the three

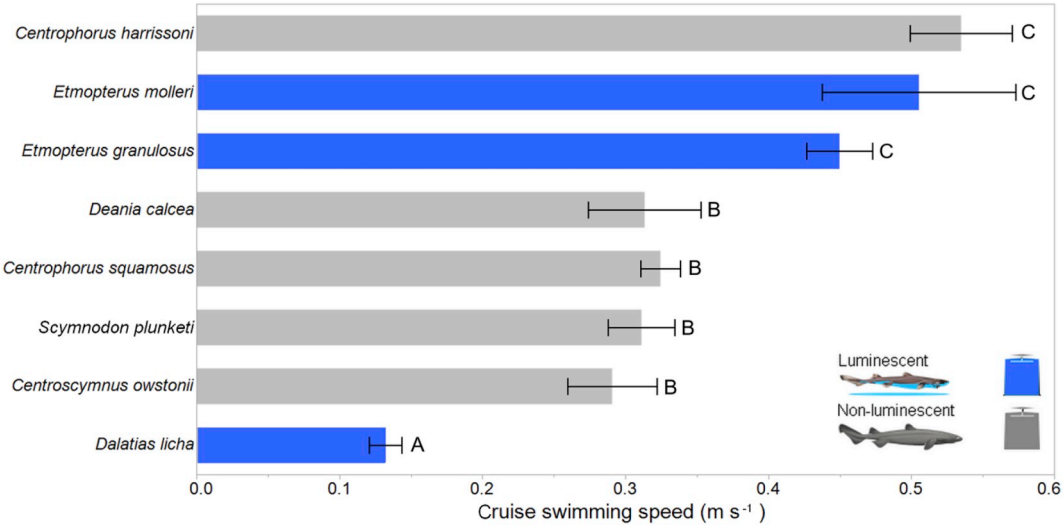

Fig. 2. Mean cruise swimming speed (m.s^{-1} $\pm$ SE) in deep-sea shark species measured by stereo-BRUVs; different capital letters indicate significant differences of cruise swimming speeds (Tukey test <0.05). Blue bars correspond to luminous deep-sea sharks, while grey bars correspond to non-luminous ones. (For interpretation of the references to colour in this figure legend, the reader is referred to the Web version of this article.)

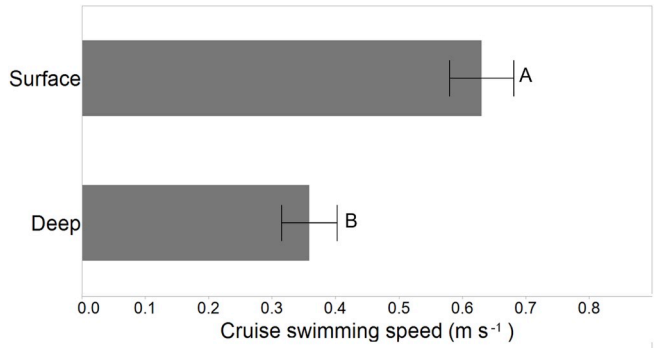

Fig. 3. Mean cruise swimming speed (m.s^{-1} ± SE) difference between deep-sea sharks (Deep) and shallow-sea sharks (Surface); different capital letters indicate significant differences (Student *t*-test <0.05). N = 20 number of surface species and N = 9 number of deep sea sharks species.

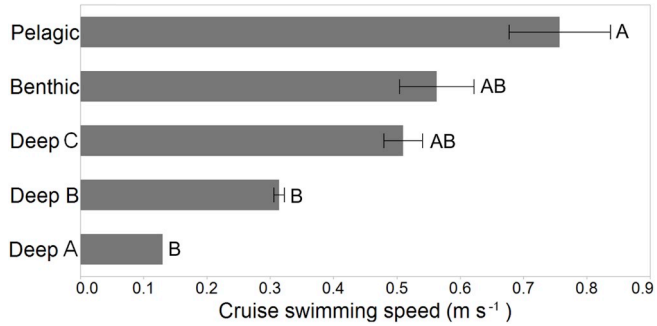

Fig. 4. Mean cruise swimming speeds (m.s^{-1} ± SE) of pelagic shallow-water sharks, benthic shallow-water sharks and deep-sea sharks. Deep-sea sharks are classified into three groups (C > B > A) based on their average swimming speed (Fig. 2). Different capital letters indicate significant differences (Tukey test <0.05). N = 13 for Benthic species, N = 7 for Pelagic species, N = 3 for Deep C, N = 5 for Deep B and N = 1 for Deep A.

groups of deep-sea sharks identified on Fig. 2 (ANOVA, $P < 0.0024$). However, post-hoc Tukey test separated sharks cruising swimming speeds into three groups: the first, with the highest value (n = 7, 0.75 ± 0.08), were the pelagic sharks; the second, benthic shallow water sharks and deep-sea sharks from velocity group Deep C (n = 13, 3; 0.56 ± 0.06; 0.51 ± 0.03, respectively); and the third group, with the lowest cruise swimming speed value (n = 5, 1; 0.31 ± 0.008; 0.13, respectively), deep-sea sharks from velocity groups Deep A and Deep B (Fig. 4).

A linear model described the relationship between the cruise swimming speed of sharks as a function of tail beat frequency, species and tail beat frequency/species interaction. There was a significant effect of each factor (tail beat frequency, species and tail beat frequency/species on the velocity) (LM, r2 = 0.71, P < 0.0001) (Fig. 5). This model showed that, for a given speed (0.3 and 0.6 m s^{-1} chosen because it fits with the minimum and the maximum velocity of the majority of deep-sea sharks, dotted lines on Fig. 5), *E. granulosus* and *E. molleri* had a higher tailbeat frequency than other deep-sea species; the mean frequency at 0.3 m s^{-1} is 0.5 Hz for most deep sea species while it reached about 1 Hz for Etmopteridae. Again at 0.6 m s^{-1} the mean was close to 0.65 Hz for most of the deep sea species while it was 1.45 Hz for Etmopteridae. Comparison of regression line slopes revealed that, in comparison to other deep-sea sharks, Etmopteridae species needed a larger increase of their tailbeat (shown by a slope <0.5) to increase their speeds. For a given speed of 0.3 m s^{-1}, the stride length was lower for the two Etmopteridae species (0.29 and 0.35 body length), higher for *Scymnodon plunketi* and *Centrophorus squamosus* (0.72 and 0.63 body length respectively) and other species displayed intermediate values (Table 2).

Linear regression on each species does not show any evidence of a relationship between cruise swimming speed and the total length of the shark.

Finally, regarding burst activities, only four species showed behavior

Table 2
Tail beat frequencies (Hz) and stride lengths (body length) for a given cruise swimming speed (0.3 m s^{-1}) for eight deep-sea shark species from Squaliformes order.

Species	Cruise swimming speed (m s^{-1})	Tail beat frequency (Hz)	Stride length (body length)
Scymnodon plunketi	0.3	0.42	0.72
Deania calcea	0.3	0.56	0.53
Centrophorus squamosus	0.3	0.48	0.63
Centroscymnus owstonii	0.3	0.62	0.48
Dalatias licha	0.3	0.59	0.51
Centrophorus harrisoni	0.3	0.61	0.49
Etmopterus granulosus	0.3	0.87	0.35
Etmopterus molleri	0.3	1.04	0.29

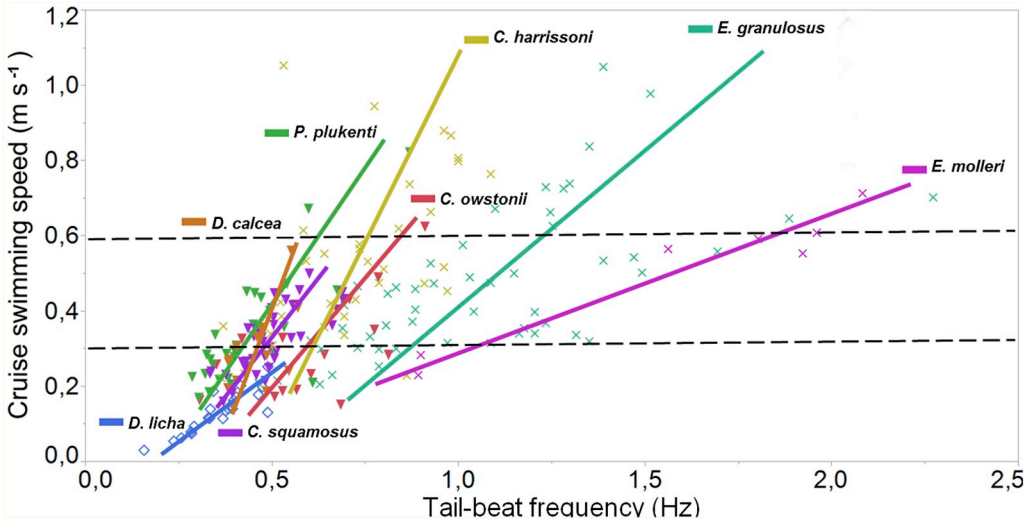

Fig. 5. Relationship between tail beat frequency (Hz) and cruise swimming speed (m s^{-1}) for eight Squaliformes deep-sea shark species. The line represents the linear regression; pink: *E. molleri*, turquoise: *E. granulosus*, red: *C. owstonii*, orange: *D. calcea*, yellow: *C. harrissoni*, purple: *C. squamosus*, green: *P. plukenti*, blue: *D. licha*; the ◊, ▼ and x correspond respectively to sharks from the group Deep A, Deep B and Deep C; the two dotted lines correspond from to 0.3, 0.6 m s^{-1} respectively. (For interpretation of the references to colour in this figure legend, the reader is referred to the Web version of this article.)

in agreement with the burst definition (Table 1). Behaviors producing burst activities were often hunting activities for *C. owstonii*, *P. plukenti* and *D. calcea*, while the small lanternshark, *E. granulosus*, had more burst activities triggered by escaping behaviors.

4. Discussion

4.1. Biodiversity, length, and aggregation

Our results showed a clear prevalence of species of Squaliformes in New Zealand deep-sea waters at 300–1200m, where they represented more than 91% of all shark occurrences observed. It is in this deep layer that the shark species richness increased to reach its maximum at 700m. Thanks to video analyses, the vertical range of one species is increased by the present study: *Scymnodon macracanthus* was observed at 300m, while its minimum depth was previously reported as 545m (Stewart and Last, 2015). Based on the most recent classification of Squaliformes in New Zealand (Roberts et al., 2015), our data reveal a shift of families starting at 300m depth, where the number of sharks from Squalidae decreased, while sharks from Somniosidae and Centrophoridae increased. In contrast, during this shift, the proportion of sharks from Etmopteridae did not change. Squalidae, Centrophoridae and Somniosidae sharks are relatively similar in terms of size, morphology, diet, and trophic level; while Etmopteridae sharks are smaller and are sometimes hunted by these first three families (Ebert et al., 2013; Pethybridge et al., 2012). Therefore, the shift observed could avoid competition between close counterparts sharing potentially the same trophic role. It is important to mention that the number of all counted Centrophoridae and Somniosidae were lower than the number of Squalidae, which is logical because food availability decreases with depth.

Regarding size measurements collected, except for *C. harrissoni*, no significant effect of depth and velocity could be found for species taken individually. This observed lack of relationship could be explained theoretically by experimenter selection, the video quality, and also light intensity. Indeed, to collect data, the chosen points of reference for length measurement should be easy to localize for all individuals. However, it was easier to label these points of reference on big sharks, rather than small ones. Therefore, there is a shift to bigger sharks observed in our study. Nevertheless, we observed three different size distribution modes, depending on the species. Moreover, the significant relationship between the three different morphometric lengths shows that, in big specimens, the measurements taken are very accurate.

Finally, *E. granulosus* occurrence revealed that this species is always present in higher number of individuals, around twelve, than other species where only two - three are observed. . Nevertheless, it was already described from fishing surveys that this species as an aggregative behavior (Finucci et al., 2018). Therefore, our results are consistent with previous findings in literature but with non-destructive methodology.

4.2. Swimming speed

In our study, the swimming speeds of several deep-sea sharks were measured for the first time *in situ*, bringing some new insights about their ecology. *In situ* measurements remain the best way to characterize organisms in their environment but bias might be possible due to environment fluctuations. Indeed, here the velocity of sharks were measured in deep-sea water where the current was not taken into account and our results should be consider this way with all environmental factors influencing sharks. However, bias should be considered minimal in our conditions since: (i) presence of weaker currents at greater depth are well known (Heath, 1972); (ii) video footages showed that every time the sediment was disturbed (i.e. when the set-up landed on the bottom or when numerous hagfishes attacked the bait or even during strong interactions between larger organisms), it took more than ten minutes for the silt and sand to sediment; what suggest low or no current. Previously, deep-sea sharks were considered as slow and lazy swimmers compared with their shallow-water counterparts. These conclusions come from indirect measurement of their metabolism. Authors argue this conclusion mainly by the cold water effect of the environment, but also because they do not need a high velocity for prey capture in dark environments (visual interaction hypothesis) (Condon et al., 2012; Treberg et al., 2003). Studies on sharks' buoyancy also show that deep-sea shark with liver providing more buoyancy is ideal adaptation for slow swimmer (Pinte et al., 2019; Gleiss et al., 2017). Our results confirmed the conclusions of previous studies, with deep-sea shark species swimming at slower cruise speeds than their shallow-water counterparts. However, the results of our study allow us to refine a hypothesis on these broad patterns because the swimming speed of deep-sea sharks inferred is clearly not uniform. Some groups of species displayed higher cruise swimming speeds than others, with the high speed group (*C. harrissoni*, *E. granulosus* and *E. molleri*; group Deep C) even showing swimming abilities comparable to benthic shallow-water sharks while pelagic shallow-water sharks remain the fastest species (See data from Ryan et al., 2015 and Watanabe et al., 2012).

These differences in cruise swimming speed between deep-sea species could be related to their living mode. In group Deep C (Fig. 2), two of the three sharks were luminous sharks from family Etmopteridae. Like other lanternsharks, *E. granulosus* and *E. molleri* have thousands of ventral photogenic organs called photophores that produce blue-green light (Claes and Mallefet, 2009a). This bioluminescence has been shown to be primarily involved in camouflage through counter-illumination, producing light on the ventral side of the animal at the same intensity, wavelength, and angular distribution as residual down-welling light of its environment. This ventral bioluminescence hides their silhouette from below (Claes and Mallefet, 2014; Claes et al., 2010). Luminous organisms must be able to change ventral light intensity quickly to be efficient counter-illuminators (Latz, 1995; Case et al., 1977; Young and Roper, 1976; Clarke, 1963). However, the luminescence of lanternsharks is under hormonal control, which is relatively slow in comparison with nervous control, as seen in many other counter-illuminating organisms (Duchatelet et al., 2019; Claes and Mallefet, 2015; Claes et al., 2011). To compensate for this slow adapting control system, it is possible that luminous deep-sea sharks have to move up and down the water column to align their ventral light intensity with their environment; this is the postulate of the "isolume followers' hypothesis" (Claes and Mallefet, 2014). Being a fast swimmer would then represent a significant adaptive advantage if these sharks perform this behavior. Vertical movement of lanternsharks is also supported by the observation of circadian migration for other species of Etmopteridae (Xavier and Vieira, 2012; Neiva et al., 2006) and stomach content analyses which revealed fishes and squids from shallower layers (Daley et al., 2002). However, this circadian migration and the presence of food from near the surface, is also observed for non-luminous deep-sea sharks, such as *Centrophorus harrissoni* (group Deep C) and *Centrophorus squamosus* (group Deep B), suggesting that other reasons exist for differences in swimming abilities of deep-sea sharks.

In contrast, *Dalatias licha* displayed the slowest cruise swimming speed ever measured for a shark, i.e. lower than the Greenland shark, *Somniosus microcephalus* (Watanabe et al., 2012). *D. licha* is assumed to be luminescent since ventral photophores were described (Straube et al., 2015), supporting the hypothesis that ventral luminescence might be used to light up the ocean floor while searching preys. Therefore, its luminescence would be useful to hunt, rather than for predation avoidance, since it is a relatively large species (attaining 185 cm TL) and unlikely to have many predators. In this context, this species is not assumed to be an "isolume-follower" as it displays a benthic living mode while Etmopteridae are bentho-pelagic species. Moreover, *D. licha* is not known to perform circadian cycle since fishing reports and stomach contents revealed that this shark remains at the same depth, feeding mainly on benthic organisms (Jones Emma, personal comm.; Daley et al., 2002). Surprisingly, fast lanternsharks are often found in *D. licha*

stomach contents (Navarro et al., 2014), what suggests that it has better burst capabilities allowing a slow and discrete approach towards its prey, before hitting fast when close as it has been observed on one footage (see Zintzen et al., 2011 for footage and description of this attack).

Our results also showed that the tail beat frequency of deep-sea shark species was positively correlated with their cruise swimming speed, which agrees with literature (Graham et al., 1990; Bainbridge, 1958). Except for the two Etmopteridae, the deep-sea shark tail beat frequency was not higher than 1 Hz, while it is often more than 1 Hz for shallow-water species (Graham et al., 1990). Our results revealed that Etmopteridae species displayed higher tail beat for a given speed than other deep-sea sharks, and that they also increase their tailbeat faster when they need to increase their cruise swimming speed. Regarding the stride length, Etmopteridae species showed the lowest values which agree with the literature on fish swimming stating that higher tail beat frequency means lower stride length. However, stride length also depends on swimming type and body shape, therefore it is species dependent. Indeed, *D. licha* which had the lowest tail beat frequency did not have the highest stride length (Svendsen et al., 2016; Videler and Wardle, 1991). One species, *C. harrissoni*, displayed a counterintuitive pattern: it presents a similar regression line to *D. licha*, while its cruise swimming speed placed it in the fastest group. One possible explanation relies on the morphology of its caudal fin. Indeed, this species had a higher proportion of the caudal region (20% of the total length – see supplementary data 2) than for the other deep-sea sharks studied. These results suggest that Etmopteridae sharks reach high-velocity due to higher tail beat frequency, which are probably related to their metabolism and muscular properties, while *C. harrissoni* goes faster due to the efficiency of its caudal fin. More work will, however, be necessary to better understand swimming abilities of deep-sea sharks using a combination of both morphological and physiological features (work in progress).

Funding

The present work was supported by a grant from the Fonds de la Recherche Scientifique (FRS-FNRS, Belgium) to N.P. & J.M. J.M. is research associate FNRS. Substantial fieldwork in offshore waters of New Zealand deploying buoyed stereo-BRUVs and fish traps was funded by a Royal Society of New Zealand Marsden Fund grant (MAU0713) and Te Papa Collection Development Programme (AP3126).

Author contribution

N.P. participated at the conceptualization, the methodology making, the formal analyses, and provided the funding for this research. U.M. was a master student helping during all the formal analyses. V.Z. and C. R. from Te Papa conceptualized and realized all steps of the fieldwork BRUVs deployed in New Zealand and provided all videos with deep-sea sharks. P.P. and C.V. from the ICTEAM-ELEN, helped for the script creation allowing the 3D measurement of size and speed. The initial draft of this manuscript was written by N.P. and was reviewed by U.M., V.Z., C.R. and J.M.

Ethical issues

For this kind of analyses ethical issues were not applicable.

Declaration of competing interest

The authors declare that they have no known competing financial interests or personal relationships that could have appeared to influence the work reported in this paper.

Acknowledgements

Firstly, we thank the crew of MV *Tranquil Image*, N. Furley, G. Gibbs and S. Kelly, who helped to organize fieldwork using baited underwater video units and fish traps. E. Harvey provided gear and expertise for the stereo-BRUVs setup. C. Struthers, R. Crech'riou, A. Smith, C. Bedford, O. Hannaford, J. Williams, J. Barker, C. Struthers and K. Rodgers also contributed to the sampling effort. E. Myers contributed to fish identifications and counts from stereo-BRUVs imagery during an internship at Te Papa. Access to shark video footage was facilitated by MJ Anderson (Massey University, Auckland); P. Last and C. Duffy helped with certain species identifications from video footage. Finally, we also thank Catherine Rasse from the statistical department of UCLouvain for help and reviewing all statistical analyses of this work.

Appendix A. Supplementary data

Supplementary data can be found online with the Elsevier version.

References

Andrews, K.S., Williams, G.D., Farrer, D., Tolimieri, N., Harvey, C.J., Bargmann, G., Levin, P.S., 2009. Diel activity patterns of sixgill sharks, Hexanchus griseus: the ups and downs of an apex predator. Anim. Behav. 78 (2), 525–536.

Bagley, P.M., Smith, A., Priede, I.G., 1994. Tracking movements of deep demersal fishes, *Coryphaenoides (Nematonurus) armatus, Antimora rostrata* and *Centroscymnus coelolepis* in the Porcupine Seabight, NE Atlantic Ocean. J. Mar. Biol. Assoc. U. K. 74, 473–480.

Bainbridge, R., 1958. The speed of swimming of fish as related to size and to the frequency and amplitude of the tail beat. J. Exp. Biol. 35 (1), 109–133.

Bernal, D., Smith, D., Lopez, G., Weitz, D., Grimminger, T.A.D.K., Dickson, K., Graham, J. B., 2003. Comparative studies of high performance swimming in sharks II. Metabolic biochemistry of locomotor and myocardial muscle in endothermic and ectothermic sharks. J. Exp. Biol. 206 (16), 2845–2857.

Case, J.F., Warner, J., Barnes, A.T., Lowenstine, M., 1977. Bioluminescence of lantern fish (Myctophidae) in response to changes in light intensity. Nature 265 (5590), 179–181.

Chiswell, S.M., Bostock, H.C., Sutton, P.J., Williams, M.J., 2015. Physical oceanography of the deep seas around New Zealand: a review. New Zeal J Mar Fresh 49 (2), 286–317.

Claes, J.M., Mallefet, J., 2009a. Hormonal control of luminescence from lantern shark (*Etmopterus spinax*) photophores. J. Exp. Biol. 212, 3684–3692.

Claes, J.M., Aksnes, D.L., Mallefet, J., 2010. Phantom hunter of the fjords: camouflage by counterillumination in a shark (*Etmopterus spinax*). J. Exp. Mar. Biol. Ecol. 388, 28–32.

Claes, J.M., Sato, K., Mallefet, J., 2011. Morphology and control of photogenic structures in a rare dwarf pelagic lantern shark (*Etmopterus splendidus*). J. Exp. Mar. Biol. Ecol. 406 (1), 1–5.

Claes, J.M., Mallefet, J., 2014. Ecological functions of shark luminescence. J. Biol. Chem. Lumin. 29, 13–15.

Claes, J.M., Mallefet, J., 2015. Comparative control of luminescence in sharks: new insights from the slender tail lantern shark (*Etmopterus molleri*). J. Exp. Mar. Biol. Ecol. 467, 87–94.

Clarke, M.W., Connolly, P.L., Bracken, J.J., 2002. Age estimation of the exploited deepwater shark Centrophorus squamosus from the continental slopes of the Rockall Trough and Porcupine Bank. J. Fish Biol. 60, 501–514.

Clarke, W.D., 1963. Function of bioluminescence in mesopelagic organisms. Nature 198, 1244–1246.

Coelho, R., Erzini, K., 2010. Depth distribution of the velvet belly, Etmopterus spinax, in relation to growth and reproductive cycle: the case study of a deep-water lantern shark with a wide-ranging critical habitat. Mar. Biol. Res. 6 (4), 381–389.

Condon, N.E., Friedman, J.R., Drazen, J.C., 2012. Metabolic enzyme activities in shallow-and deep-water chondrichthyans: implications for metabolic and locomotor capacity. Mar. Biol. 159 (8), 1713–1731.

Daley, R.K., Stevens, J.D., Graham, K.J., 2002. Catch analysis and productivity of the deepwater dogfish resource in southern Australia. CSIRO Mar Res.

Duchatelet, L., Claes, J.M., Mallefet, J., 2019. Embryonic expression of encephalopsin supports bioluminescence perception in lanternshark photophores. Mar. Biol. 166 (2), 21. https://doi.org/10.1007/s00227-019-3473-9.

Ebert, D.A., Fowler, S.L., Compagno, L.J., 2013. Sharks of the World: a Fully Illustrated Guide. Wild Nature Press, Plymouth, England.

Finucci, B., Dunn, M.R., Jones, E.G., 2018. Aggregations and associations in deep-sea chondrichthyans. ICES J. Mar. Sci. 75 (5), 1613–1626.

Gallo, N., Cameron, J., Hardy, K., Fryer, P., Bartlett, D., Levin, L., 2014. Submersible-and lander-observed community patterns in the Mariana and New Britain trenches: influence of productivity and depth on epibenthic and scavenging communities. Deep Sea Res Part 1 Oceanogr Res Pap 99, 119–133.

Gemballa, S., Konstantinidis, P., Donley, J.M., Sepulveda, C., Shadwick, R.E., 2006. Evolution of high-performance swimming in sharks: transformations of the musculotendinous system from subcarangiform to thunniform swimmers. J. Morphol. 267 (4), 477–493.
Girard, M., Du Buit, M.H., 1999. Reproductive biology of two deep-water sharks from the British Isles, Centroscymnus coelolepis and Centrophorus squamosus (Chondrichthyes: Squalidae). J. Mar. Biol. Assoc. U. K. 79 (5), 923–931.
Gleiss, A.C., Potvin, J., Goldbogen, J.A., 2017. Physical trade-offs shape the evolution of buoyancy control in sharks. Proc. R. Soc. B. Biol. Sci. 284 (1866), 20171345.
Graham, J.B., DeWar, H., Lai, N.C., Lowell, W.R., Arce, S.M., 1990. Aspects of shark swimming performance determined using a large water tunnel. J. Exp. Biol. 151 (1), 175–192.
Hartley, R., Zisserman, A., 2004. Multiple View Geometry in Computer Vision, second ed. Cambridge University Press.
Heath, R.A., 1972. Choice of reference surface for geostrophic currents around New Zealand. New Zeal J Mar Fresh 6 (1–2), 148–177.
Heikkilä, J., 2000. Geometric camera calibration using circular control points. IEEE Trans. Pattern Anal. Mach. Intell. 22 (10).
Heikkilä, J., Silken, O., 1997. A four-step camera calibration procedure with implicit image correction. IEEE Comput Soc Conf Comput Vis Pattern Recognit 97, 1106.
Lauder, G.V., Di Santo, V., 2015. Swimming mechanics and energetics of elasmobranch fishes. Fish Physiol. 34, 219–253.
Latz, M.I., 1995. Physiological mechanisms in the control of bioluminescent countershading in a midwater shrimp. Mar. Freshw. Behav. Physiol. 26 (2–4), 207–218.
Navarro, J., López, L., Coll, M., Barría, C., Sáez-Liante, R., 2014. Short-and long-term importance of small sharks in the diet of the rare deep-sea shark *Dalatias licha*. Mar. Biol. 161 (7), 1697–1707.
Neiva, J., Coelho, R., Erzini, K., 2006. Feeding habits of the velvet belly lanternshark *Etmopterus spinax* (Chondrichthyes: Etmopteridae) off the Algarve, southern Portugal. J. Mar. Biol. Assoc. U. K. 86, 835–841, 04.
Nelson, D.R., McKibben, J.N., Strong, W.R., Lowe, C.G., Sisneros, J.A., Schroeder, D.M., Lavenberg, R.J., 1997. An acoustic tracking of a megamouth shark, Megachasma pelagios: a crepuscular vertical migrator. Environ. Biol. Fish. 49 (4), 389–399.
Pethybridge, H., Butler, E.C.V., Cossa, D., Daley, R., Boudou, A., 2012. Trophic structure and biomagnification of mercury in an assemblage of deepwater chondrichthyans from southeastern Australia. Mar. Ecol. Prog. Ser. 451, 163–174.
Pinte, N., Godefroid, M., Abbas, O., Baeten, V., Mallefet, J., 2019. Deep-sea sharks: relation between the liver's buoyancy and red aerobic muscle volumes, a new approach. Comp. Biochem. Physiol. Mol. Integr. Physiol. 236 https://doi.org/10.1016/j.cbpa.2019.06.020.
Roberts, C.D., Stewart, A.L., Struthers, C.D., 2015. The Fishes of New Zealand, two. Te Papa Press, Wellington, New Zealand, 1–576.
Rodríguez-Cabello, C., González-Pola, C., Sánchez, F., 2016. Migration and diving behavior of *Centrophorus squamosus* in the NE Atlantic. Combining electronic tagging and Argo hydrography to infer deep ocean trajectories. Deep Sea Res Part 1 Oceanogr Res Pap 115, 48–62.
Rodríguez-Cabello, C., Sánchez, F., 2014. Is *Centrophorus squamosus* a highly migratory deep-water shark? Deep Sea Res Part 1 Oceanogr Res Pap 92, 1–10.
Ryan, L.A., Meeuwig, J.J., Hemmi, J.M., Collin, S.P., Hart, N.S., 2015. It is not just size that matters: shark cruising speeds are species-specific. Mar. Biol. 162 (6), 1307–1318.
Sainte-Marie, B., Hargrave, B.T., 1987. Estimation of scavenger abundance and distance of attraction to bait. Mar. Biol. 94 (3), 431–443.
Shadwick, R., Farrell, A., Brauner, C., 2016. Physiology of Elasmobranch Fishes: Structure and Interaction with Environment. Janice Audet, London.
Shadwick, R.E., Goldbogen, J.A., 2012. Muscle function and swimming in sharks. J. Fish Biol. 80 (5), 1904–1939.
Stewart, A.L., Last, P.R., 2015. Family Somniosidae', pages 148–161. In: Roberts, C.D., Stewart, A.L., Struthers, C.D. (Eds.), The Fishes of New Zealand, two. Te Papa Press, Wellington, New Zealand.
Straube, N., Li, C., Claes, J.M., Corrigan, S., Naylor, G.J., 2015. Molecular phylogeny of Squaliformes and first occurrence of bioluminescence in sharks. BMC Evol. Biol. 15 (1), 162.
Svendsen, M.B., Domenici, P., Marras, S., Krause, J., Boswell, K.M., Rodriguez-Pinto, I., et al., 2016. Maximum swimming speeds of sailfish and three other large marine predatory fish species based on muscle contraction time and stride length: a myth revisited. Biology open 5 (10), 1415–1419.
Thomson, K.S., Simanek, D.E., 1977. Body form and locomotion in sharks. Am. Zool. 17 (2), 343–354.
Treberg, J.R., Martin, R.A., Driedzic, W.R., 2003. Muscle enzyme activities in a deep-sea squaloid shark, Centroscyllium fabricii, compared with its shallow-living relative, Squalus acanthias. J. Exp. Zool. A Comp. Exp. Biol. 300 (2), 133–139.
Videler, J.J., Wardle, C.S., 1991. Fish swimming stride by stride: speed limits and endurance. Rev. Fish Biol. Fish. 1 (1), 23–40.
Watanabe, Y.Y., Lydersen, C., Fisk, A.T., Kovacs, K.M., 2012. The slowest fish: swim speed and tail beat frequency of Greenland sharks. J. Exp. Mar. Biol. Ecol. 426, 5–11.
Wilson, S.G., Polovina, J.J., Stewart, B.S., Meekan, M.G., 2005. Movements of whale sharks (Rhincodon typus) tagged at Ningaloo Reef, Western Australia. Mar. Biol. 148 (5), 1157–1166.
Xavier, J.C., Vieira, C., et al., 2012. Feeding ecology of the deep-sea lanternshark *Etmopterus pusillus* (Elasmobranchii: Etmopteridae) in the northeast Atlantic. Sci. Mar. 76 (2), 301–310.
Young, R.E., Roper, C.F., 1976. Bioluminescent countershading in midwater animals: evidence from living squid. Science 191 (4231), 1046–1048.
Zhang, Z., 1999. Flexible camera calibration by viewing a plane from unknown orientations. In: Proc IEEE Int Conf Comput Vis.
Zintzen, V., Roberts, C.D., Anderson, M.J., Stewart, A.L., Struthers, C.D., Harvey, E.S., 2011. Hagfish predatory behaviour and slime defence mechanism. Sci. Rep. 1, 131.
Zintzen, V., Anderson, M.J., Roberts, C.D., Harvey, E.S., Stewart, A.L., Struthers, C.D., 2012. Diversity and composition of demersal fishes along a depth gradient assessed by baited remote underwater stereo-video. PLoS One 7 (10), e48522.
Zintzen, V., Anderson, M.J., Roberts, C.D., Harvey, E.S., Stewart, A.L., 2017. Effects of latitude and depth on the beta diversity of New Zealand fish communities. Sci. Rep. 7 (1), 8081.